



OPEN

Identification of splice regulators of fibronectin-EIIIA and EIIIB by direct measurement of exon usage in a flow-cytometry based CRISPR screen

Jessica A. Hensel¹, Brent D. Heineman¹, Amy L. Kimble¹, Evan R. Jellison², Bo Reese³ & Patrick A. Murphy^{1,4}✉

The extracellular matrix protein fibronectin (FN) is alternatively spliced in a variety of inflammatory conditions, resulting in increased inclusion of alternative exons EIIIA and EIIIB. Inclusion of these exons affects fibril formation, fibrosis, and inflammation. To define upstream regulators of alternative splicing in FN, we have developed an in vitro flow-cytometry based assay, using RNA-binding probes to determine alternative exon inclusion level in aortic endothelial cells. This approach allows us to detect exon inclusion in the primary transcripts themselves, rather than in surrogate splicing reporters. We validated this assay in cells with and without FN-EIIIA and -EIIIB expression. In a small-scale CRISPR KO screen of candidate regulatory splice factors, we successfully detected known regulators of EIIIA and EIIIB splicing, and detected several novel regulators. Finally, we show the potential in this approach to broadly interrogate upstream signaling pathways in aortic endothelial cells with a genome-wide CRISPR-KO screen, implicating the TNF α and RIG-I-like signaling pathways and genes involved in the regulation of fibrotic responses. Thus, we provide a novel means to screen the regulation of splicing of endogenous transcripts, and predict novel pathways in the regulation of FN-EIIIA inclusion.

Alternative splicing of the essential extracellular matrix protein fibronectin (FN) is tightly regulated during development and in disease¹. Increased inclusion of alternative exons EIIIA(EDA) and EIIIB(EDB) in the vascular ECM and the circulation coincides with a range of human diseases involving endothelial activation and increased risk of thrombosis and fibrosis, including acute traumatic injury^{2,3} and chronic responses—as in type II diabetes^{4,5}. Within the vasculature, and in sites of fibrosis, the endothelium is a key source of FN and the FN splice isoforms^{6,7}. Germline deletion of alternative spliced exons EIIIA(EDA) and EIIIB(EDB) leads to lethal vascular defects in development on some genetic backgrounds⁸, and surviving mice exhibit impaired vascular remodeling and risk of vascular hemorrhage^{8–12}. Genetic deletion of the EIIIA exon alone reduces clot formation^{13,14} and fibrotic responses in the skin^{6,15}, liver¹⁶, lung¹⁷, and in heart attack¹⁸ and stroke models¹⁴. Thus, EIIIA and EIIIB inclusion is tightly regulated, and is associated with vascular remodeling, thrombosis and fibrosis.

We showed that EIIIA and EIIIB inclusion in the endothelium increases in response to hematopoietic cell recruitment, but the molecular mediators are not yet clear^{12,19}. TGF β is an important mediator of endothelial EIIIA inclusion in fibrotic responses in the liver^{7,20}; however, there are likely other molecular mediators as well. In other cell types, extracellular cues regulating EIIIA inclusion include basement membrane proteins²¹, and growth factors such as HGF²². PI3K signaling is an important intracellular mediator EIIIA and EIIIB induction in some contexts^{23–25}, leading to increased activity of splice factor phosphorylation and activation. Serine and arginine rich splicing factors (e.g. SRSF1, -3, -5, and -7) promote EIIIA and EIIIB inclusion in an apparently additive manner^{26–28}. In contrast to the redundant activities SRSF proteins on EIIIA and EIIIB inclusion, the splice factor Rbfox2 is essential for EIIIB inclusion in multiple cell types^{19,29}, and also has an important role in

¹Center for Vascular Biology, UCONN Health, Farmington, CT, USA. ²Department of Immunology, UCONN Health, Farmington, CT, USA. ³Institute for Systems Genomics - Center for Genome Innovation, UCONN, Storrs, CT, USA. ⁴Center for Vascular Biology & Calhoun Cardiology Center, University of Connecticut Medical School, 263 Farmington Avenue, Farmington, CT 06030, USA. ✉email: pamurphy@uchc.edu

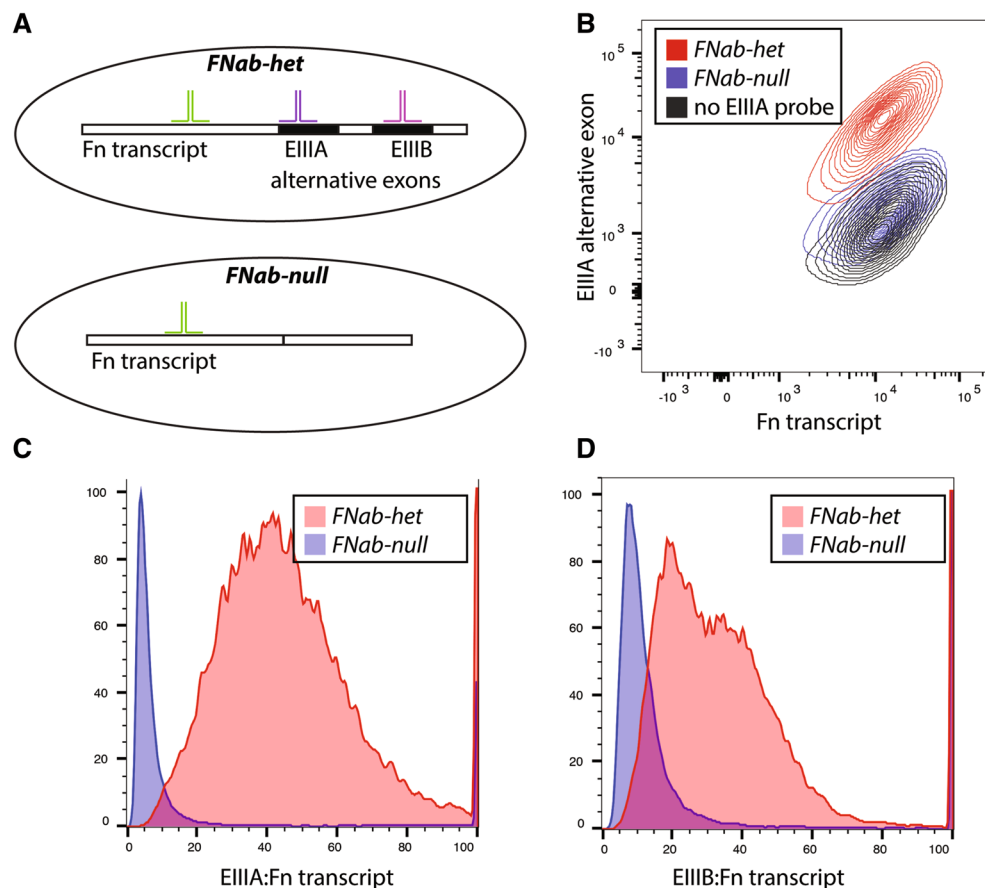


Figure 1. RNA-hybridization assay to measure inclusion of fibronectin alternative exons in individual endothelial cells. **(A)** Schematic showing binding of probes to transcripts containing EIIIA (from *FNab-het* cells) or not (from *FNab-null* cells). Probes to the constitutive region of FN bind to both transcripts (green), but probes to EIIIA (purple) or EIIIB (pink) binds only to these alternatively spliced exon (black region of FN transcript) when they are included in cells. **(B)** Fluorescent flow cytometry plot showing fluorescence detected in all cells for the FN probe (x-axis), but only detected for the EIIIA probe (y-axis) in cells expressing FN with EIIIA (red). Signal is absent when no EIIIA probe is included (but fluorescent detection is still performed, black), or when cells do not produce the EIIIA inclusive FN transcript (blue). **(C,D)** Ratio of signal from EIIIA probe **(A)** or EIIIB probe **(B)** to total FN probe from flow cytometry as in **(B)**.

EIIIA induction in the arterial endothelium¹⁹. Nevertheless, knowledge of upstream mediators of EIIIA and EIIIB inclusion is still incomplete.

Here, we describe an approach to assess RNA splicing in native transcripts with single cell resolution, and show how this approach allows for the screening of upstream mediators of EIIIA and EIIIB inclusion in cultured aortic endothelial cells. We validate that this approach identifies known regulators of EIIIA and EIIIB splicing in a targeted screen, and use the approach in a genome-wide screen to identify novel genetic dependencies.

Results

Direct measurement of FN splicing variants using fluorescent in situ probes. We established an assay to examine endogenous RNA splice isoforms in single cells using a commercial in situ hybridization protocol compatible with flow-cytometry (PrimeFlow). DNA oligomer probes were designed to bind the alternative fibronectin exons EIIIA and EIIIB, as well as exons in the constitutive region of Fibronectin. These probes allow sequence specific fluorescent detection of RNA by flow cytometry after signal amplification (Fig. 1A). To validate our approach, we used murine aortic endothelial cells with and without genetic deletion of the EIIIA and EIIIB exons. We found increased staining with both the EIIIA and EIIIB probes in *FnAB-het* cells, compared to *FnAB-null* cells (Fig. 1B and data not shown), indicating that our probes are specific to these domains. Importantly, there was no difference in total FN staining in the cells, showing that the reduced signal is specific to the splice domains within the FN transcript (Fig. 1B). Notably, our results indicate very little background signal from the EIIIA and EIIIB probes in the absence of RNA substrate. The signal for both probes in *FnAB-null* cells is comparable to cells without the EIIIA or EIIIB probe (Fig. 1B). As we were most interested in the ratio of splice isoform to total FN, or the percent spliced in (Psi), we normalized EIIIA and EIIIB inclusion to total FN. We observed that there is a range of inclusion frequencies between cells, but that almost all *FnAB-het* cells have inclusion

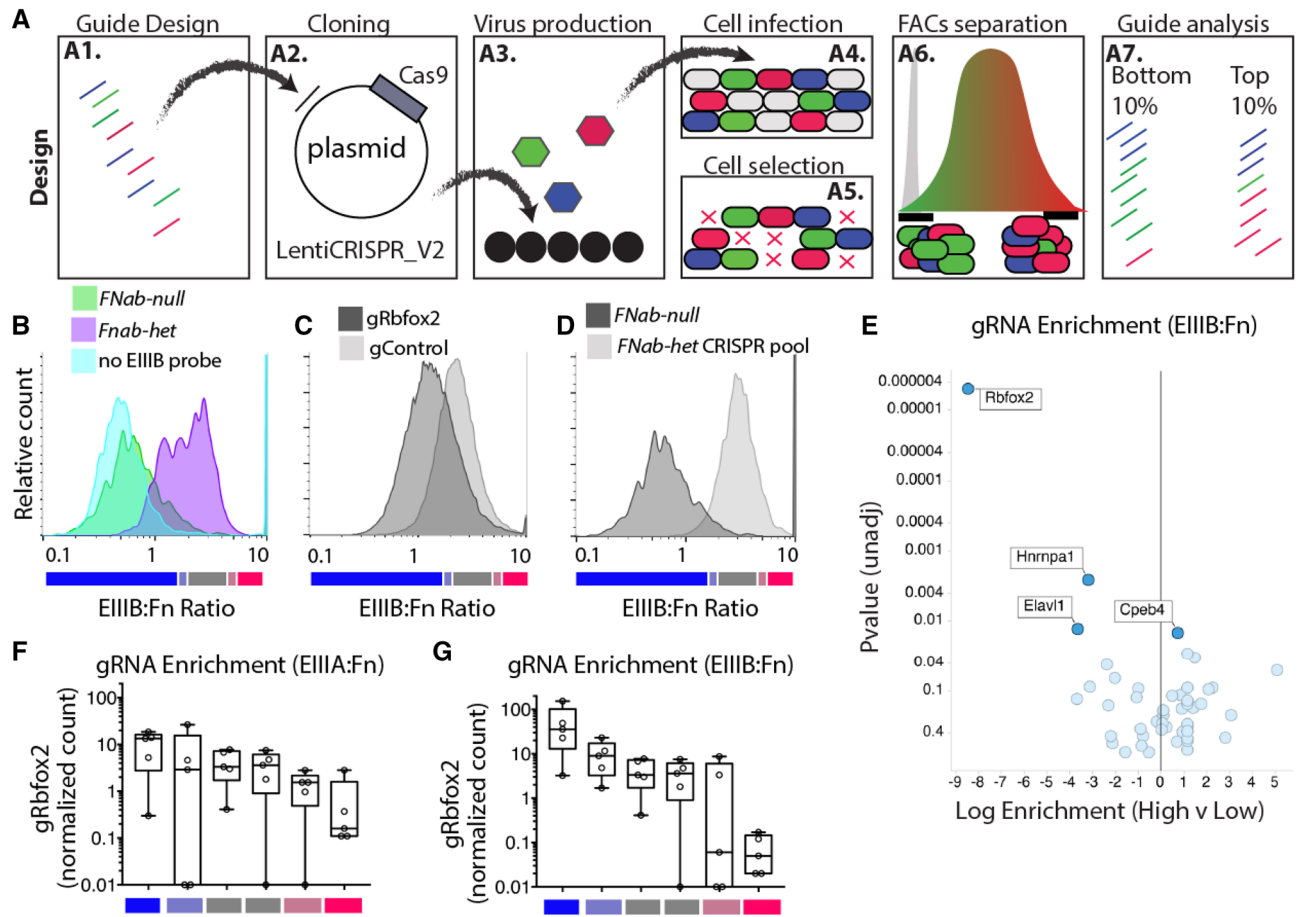


Figure 2. Application of CRISPR screening approach to define regulators of EIIIA and EIIIB inclusion. **(A)** Screening approach (A1) Guides to each target gene of interest were designed using the latest rules in the Broad design tool, and prepared as an ssDNA oligo pool. Low-cycle PCR generates dsDNA with ligation sites for (A2) batch cloning into a lentiviral backbone containing Cas9 and guide expression site. (A3) The resultant plasmid library is then used for production of lentivirus and infection of cells (A4). Infection is at 0.3 MOI and (A5) selection is by puromycin. (A6) Selected cells are sorted on the inclusion of alternative exon. Cells in the top 10% and bottom 10% of the response are isolated. (A7) Genomic DNA is isolated and guide enrichment in cells is assessed by sequencing of amplified lentiviral insertions. **(B–D)** Ratio of EIIIB to Fn probes, showing cells with and without EIIIB or no EIIIB probe at all **(B)**, a guide targeting Rbfox2 (gRbfox2) or a control guide (gControl) **(C)** and the pool of CRISPR guides targeting all 57 splice factors **(D)**. **(E)** Volcano plot showing the enrichment of guides for the indicated genes among cells with high levels of EIIIB inclusion versus low levels of EIIIB inclusion. Log enrichment and p-value is from MaGeCK analysis. **(F,G)** Plots showing the normalized count for individual guides targeting Rbfox2 in each sorted group of cells. Low, mid, or high levels of EIIIA and EIIIB inclusion are shown and represent the bins shown in **(B–D)**.

levels above the no inclusion controls (FnAB-null, Fig. 1C,D). Furthermore, although we are not currently able to directly validate the correlation between splicing reporter and transcript at a single cell level, quantitative PCR analysis of isolated low and high EIIIA inclusive fractions indicate a good correlation with EIIIA to total FN transcript (SI Fig. S1). These results confirmed our methodology and provided the basis for CRISPR screening and identification of EIIIA and EIIIB regulators.

Small scale screen of candidate RBPs identifies known regulators of EIIIA and EIIIB. We had observed that EIIIA and EIIIB are co-regulated with hundreds of other skipped exons in endothelial cells activated by hematopoietic cell recruitment under low and disturbed flow^{12,19}. Hypothesizing that common upstream RNA-binding proteins (RBPs) regulate this splicing response, we had assessed flanking regions of these skipped exons to identify likely regulatory RBPs¹⁹. This identified Rbfox2, which we previously found is required for EIIIB inclusion and contributes to EIIIA inclusion in the endothelium¹⁹. However, we also identified 57 other RBPs likely active in this response (SI Fig. S2). To determine whether any of these RBPs also regulate EIIIA and EIIIB inclusion we performed a small scale CRISPR KO screen, using our in situ hybridization protocol as a readout (Fig. 2A, SI Fig. S3). Five guide RNA (gRNA) pairs were designed to each of the candidate RBPs, and constructs were generated in a pooled approach. Analysis of the plasmid pool showed good representation of each targeting construct and minimal skew across the library (SI Fig. S4A,B). Lentivirus was produced in a

pooled approach, and transduced into murine aortic endothelial cells at MOI < 0.3. A collection of cells at 3 days post-post infection (dpi) showed that representation in cells mirrored the representation in the plasmid library (SI Fig. 4B).

Having created a cellular library with constructs targeting each of our candidate RBPs, we then tested for regulation of EIIIA and EIIIB inclusion using our splicing assay. In addition to the FnAB-null cells, we included an efficient lentiviral CRISPR KO construct to Rbfox2 which reduces Rbfox2 protein and EIIIB inclusion as a control (SI Fig. S5). This resulted in the expected reduction of EIIIB inclusion, confirming that deletion of a regulatory splice factor leads to a detectable change in splicing (Fig. 2). In our CRISPR KO pool, we predicted that Rbfox2 and other gRNA targeting RBPs important in EIIIA or EIIIB inclusion would be enriched in cells with lowest inclusion levels. Conversely, we predicted that gRNA targeting RBPs suppressing EIIIA or EIIIB inclusion would be enriched in cells with highest inclusion. Therefore, we sorted the top 10%, bottom 10%, based on EIIIA or EIIIB inclusion (Fig. 2D, SI Fig. S6). We sorted 200 K cells in each pool, providing a theoretical coverage of > 700 cells per guide (SI Fig. S3). Lentiviral insertions were amplified from biological replicates of sorted populations in a nested PCR, as previously reported^{30,31}. Counting and distribution analysis with a negative binomial model was performed using MaGeCK³². As expected, we found the strongest signal for Rbfox2 as a required regulator of EIIIB, and a weaker signal as a regulator of EIIIA (Fig. 2E–G, SI Fig. S6). Also as expected, guides to Srsf5, which promotes of EIIIA inclusion, were enriched in cells with reduced EIIIA (SI Fig. S6). We confirmed this effect in cells infected with a single Srsf5 targeting lentivirus (SI Fig. S7). Together, these results confirm the detection of expected regulators, and also hint at a role for previously undescribed EIIIA and EIIIB regulators, such as Hnrnpa1 and Elavl1 (EIIIB) and Pcbp2 and Cpsf6 (EIIIA).

Genome-wide CRISPR KO screen for regulators of EIIIA inclusion. As small-scale screens identified known splice-factor regulators of EIIIA and EIIIB, we aimed to expand this approach to examine the regulation of EIIIA specifically on a genome-wide scale. We used the Brie genome-wide CRISPR-KO library³³. The plasmid library, which showed good conservation and low skew in the representation of all plasmids, was used to produce virus and infect aortic endothelial cells at > 100 cells per guide (at < 0.3 MOI), resulting in a cellular library with a skew of 30 from the top 20% to the bottom 80%, and guide coverage of > 97%. The library was kept at > 100 cells per guide coverage, and two separated pools of virus production and infection were used to generate the final pool (see SI Fig. S3). Cells were expanded over two weeks in culture, and were assessed by splicing analysis. The top 10%, bottom 10% and mid 30% of cells were isolated, based on their expression of EIIIA to total FN. Each of these populations was separated into multiple PCR reactions (see SI Table S1, SI Fig. S3), and an Illumina library was generated by nested PCR reactions.

We found that expected genes were enriched. For example, gRNAs to Rbfox2 are enriched among cells with lowest EIIIA inclusion (Fig. 3A,B). This is consistent with both the results of our small-scale screen and a reduction in EIIIA with endothelial deletion of the splice factor in vitro and in vivo¹⁹ (SI Fig. S8). Guides to Notch4 were also enriched among cells with the lowest levels of EIIIA inclusion (Fig. 3B), consistent with prior work showing that Notch4 is required for EIIIA expression in lymphatic valves in vivo, and in lymphatic endothelial cells in vitro³⁴. Guides to TGF-beta receptors were not enriched in endothelial cells with low EIIIA inclusion, suggesting that in contrast to other settings, EIIIA responses in aortic endothelial cells may not require sustained TGF-beta signaling. This is supported by our own in vitro and in vivo data showing no effect of TGF-beta inhibitors on EIIIA inclusion in these aortic endothelial cells (SI Fig. S9).

To better understand the pathways regulating EIIIA inclusion, we identified genes promoting EIIIA inclusion or EIIIA skipping based on gRNA enrichment and performed a gene set analysis of enriched genes using GSEA (Fig. 3C–F). Genes that increased EIIIA inclusion when deleted included Type II diabetes (KEGG), Stat3, and Stat5 signaling pathways (Fig. 3D,F), all of which are linked to insulin signaling responses. We found that the deleted genes linked to reduced EIIIA inclusion are concentrated in the RIG-I-like signaling pathway (KEGG), and interferon alpha response (Hallmark)—two related inflammatory pathways (Fig. 3C,E). As viral infection, which leads to RIG-I like pathway activation, induces fibrotic responses in the lung³⁴ and liver^{35,36}, we examined this interaction in more detail. We found that priming of the mouse or human endothelium by TNF α or Il1 β lead to an increase in the expression of RIG-I-like pathway components, including Dhx58, and also increased EIIIA inclusion but not total FN production (SI Fig. S10A–E). Furthermore, we found that poly:IC addition, which can trigger endothelial RIG-I-like responses, led to a further increase in EIIIA, but not EIIIB inclusion or total FN expression (SI Fig. S10F–H). We note that a similar convergence of cytokine stimulation of Poly:IC activation has also been observed in dendritic cells in the brain³⁷. Thus, treatments of aortic endothelial cells leading to increased RIG-I-like signaling pathway expression and activity can selectively increase EIIIA inclusion without increasing total FN transcript levels, consistent with a requirement for this pathway in EIIIA expression in our screen.

Genes regulating EIIIA inclusion correlate with published fibrotic phenotypes. As EIIIA inclusion is a driver of fibrotic responses, we predicted that deletion of genes which suppress EIIIA inclusion would lead to reduced fibrosis. Conversely, we expected that deletion of genes which lead to increased EIIIA inclusion would increase fibrosis. To test this, we asked whether EIIIA-regulating genes also regulate fibrotic responses in published data (Fig. 4A,B). We examined the top 100 gene deletions predicted to increase EIIIA inclusion (“High EIIIA”) or promote EIIIA skipping (“Low EIIIA”) based on the enrichment of their gRNA and an unadjusted p-value < 0.05. We performed a literature search for effects of gene deletion or suppression on fibrotic phenotypes in vivo or in vitro. We found literature support for the effects of KO or KD on fibrosis (increased or decreased) for 14% of the genes in both Group I and Group II. CRISPR-targeted genes leading to increased EIIIA inclusion (High EIIIA) were associated with increased fibrosis in KO or KD (84% increased fibrosis, Fig. 4A). The CRISPR-targeted genes

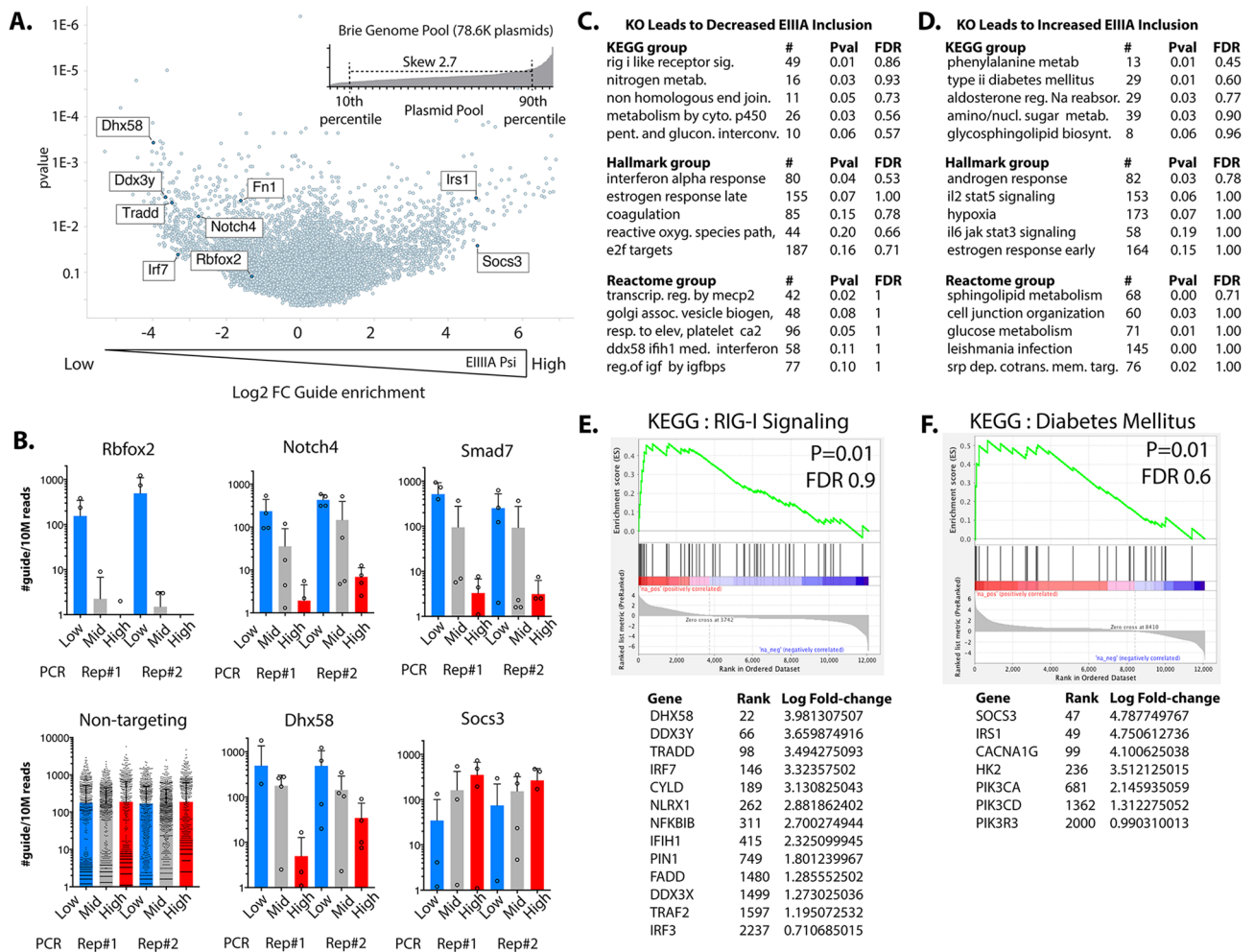


Figure 3. Genome-wide identification of EIIIA regulators. (A) Guide representation in plasmid pool (Brie library) after amplification in bacteria (inset), and volcano plot from MaGeCK analysis showing genes predicted to positively or negatively regulate EIIIA inclusion, based on the enrichment of their specific gRNA. (B) Plots showing individual guides for the genes of interest, and their relative enrichments in sorted cells with low, mid, or high levels of EIIIA inclusion. (C) GSEA analysis showing the enrichment of genes associated with specific KEGG, Hallmark and Reactome gene groups among those targeted in cells with reduced EIIIA inclusion (indicating that these genes promote EIIIA inclusion), and (D) similar analysis of genes targeted more frequently in cells with increased EIIIA inclusion (indicating that these genes suppress EIIIA inclusion). (E) Example of GSEA plot and enriched genes from (C). (F) Similar GSEA plot and enriched genes from (D). GSEA gene set enrichment, #number of genes in group. Pval unadjusted P-value, FDR false discovery rate.

which led to reduced EIIIA inclusion in our screen (Low EIIIA), KO, or KD are associated mainly with less fibrosis (71% reduced fibrosis, Fig. 4A). While we assessed only a few of the genes in our screen, we would predict that many of the other still unannotated genes will have similar effects on the fibrotic response (Fig. 4B). Thus, our data predicts genes involved in the fibrotic response in vivo and in vitro.

Discussion

Here, we validate a novel means of assessing splicing responses in individual cells by multicolor in situ hybridization and show the utility of this approach in a CRISPR KO screen for upstream regulators of EIIIA and EIIIB inclusion. This approach addresses a number of limitations with splice reporters commonly used for this type of screen by preserving contextual and chromosomal specific regulatory mechanisms closely tied to the spliceosomal machinery, and allowing the analysis of primary cells without the introduction of retroviral or plasmid splice reporter constructs. Furthermore, we harness this approach for the broad and unbiased identification of novel regulators of FN-EIIIA splicing, identifying a strong positive correlation with genes affecting fibrotic responses in published data, including the RIG-I-like signaling pathway.

Advantages and limitations of multicolor in situ hybridization over splice reporters. Our approach is the first to assess splicing changes within individual cells in a flow-cytometry based assay. To identify regulators of alternative splicing, prior work used splice reporters as a surrogate for the endogenous splicing

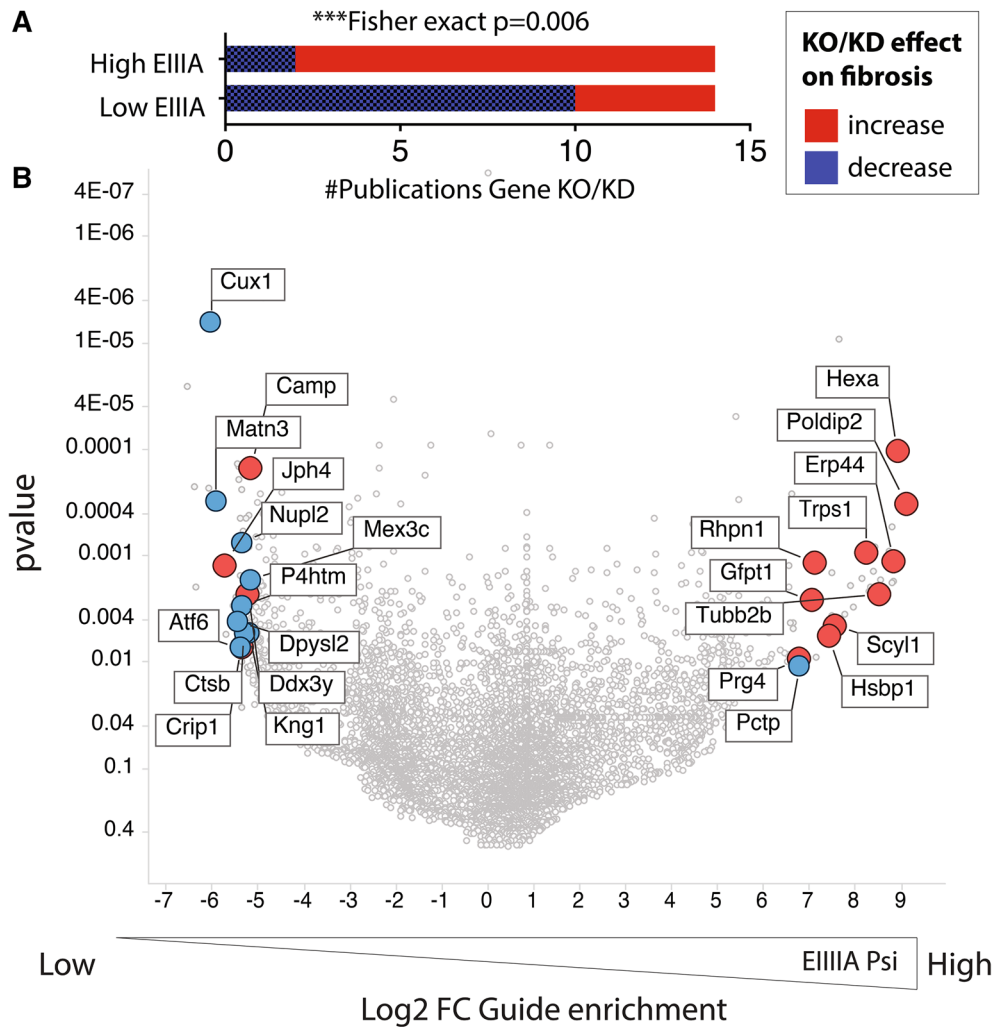


Figure 4. FN splicing regulators correlate with fibrotic phenotypes. (A,B) Analysis of top regulatory genes from CRISPR screen in publicly available data. (A) Graph showing the literature supporting either an increase or decrease in fibrotic effects in mice or cells in culture, following gene deletion or suppression. The top 100 most enriched genes in cells with either increased EIIIA inclusion or decreased EIIIA inclusion were assessed. (B) Volcano plot, showing the genes with literature support for effects on fibrotic responses, positively or negatively.

change. These reporters allow the testing of intronic and exonic sequences contributing to splicing changes, and can provide an important means of quickly screening for splicing regulators. Generally, findings from these screens are subsequently verified in the endogenous transcripts in a more physiological setting. Nevertheless, as screening tools, they suffer from a range of disadvantages that limit their accuracy as surrogates for endogenous splicing patterns, and limit the opportunity to identify endogenous splicing regulators. First, as the reporters are typically plasmid or retroviral insertions, they are size restricted, and lack the chromosomal context of the actual gene location. There are extensive interactions between gene promoters, transcriptional machinery, and RBPs regulating the spliceosome³⁸. There are also direct impacts of transcriptional regulation on RNA splicing²⁶. These factors limit a splicing reporter's ability to accurately recapitulate the contextual machinery that we know contributes to the regulation of alternative splicing. Second, RNA splicing can be regulated by long-range interactions within the mRNA itself, sometimes several kb from the regulated splicing event³⁹. Given the size limitations of splicing reporters introduced into cells, these long-range interactions are not typically considered. Third, as splice reporters must be introduced into cells, it is difficult to work with primary cells and most work has been done with plasmids in easily transfected cell lines, which may not be relevant to the cellular phenotype being modeled. Fourth, as these reporters also measure the stability of the protein readout, effects on protein stability must be carefully controlled for in assay design⁴⁰. Thus, by several measures, our direct in situ hybridization screen offers benefits over splice reporter screens.

Although in situ hybridization screening has benefits, it also has some limitations. First, this assay is capable of detecting splice isoforms only in fixed and permeabilized cells; thus, iterative screens to purify cells with most or least inclusion is not possible. Second, the splicing change must be large enough to land the oligomer probes on the novel sequence. The EIIIA and EIIIB exons are ~270 bp in length, but shorter regions would be

much more challenging. Lastly, the sensitivity of the approach depends not only on size of the targeted region, but also the copy number in the cell. This assay is reported to have a sensitivity of below 10 transcripts per cell in optimal conditions⁴¹, but given the additional size limitations, sensitivity to splice isoforms is likely less. FN is among the most expressed transcripts in our aortic endothelial cells, with expression level similar to beta-actin (by FPKM). EIIIA and EIIIB exons contribute to the majority of these transcripts in the aortic endothelial cells. Therefore, FN and the alternative exons EIIIA and EIIIB provide abundant targets for this approach. Novel methods to detect and quantify RNA transcripts in cells may be needed to adapt this assay for the analysis of lower abundance splice isoforms.

Identification of novel pathways modulating EIIIA inclusion. This new data further validates our previous discovery that Rbfox2 is a key regulator of EIIIB inclusion in arterial endothelial cells¹⁹, as it is in mouse stem cells²⁹. Here, we also show that Rbfox2 affects EIIIA inclusion, although the effects on EIIIA are not as pronounced as on EIIIB, which is also consistent with our prior observations in Rbfox2 KO mice¹⁹. Among other known regulators of FN splicing, Srsf1 and Srsf3 are notably absent, possibly due to impaired cellular growth or increased lethality caused by complete deletion. Indeed, we have found that protein expression is retained in cells with Srsf1 targeting guides, suggesting that these guides are either inactive, or more likely, that the indels they generated have retained the Srsf1 protein coding sequence (SI Fig. S6). However, Srsf5 deletion appears to be well tolerated, and its deletion suppressed EIIIA inclusion in our screen and also in cells when measured by qPCR (SI Fig. S5). While the involvement of the other pathways identified in this screen will need additional validation in vitro and in vivo, the identification of pathways activated in diabetes and RIG-I-like anti-viral responses could provide new approaches to addressing vascular fibrosis in these diseases. A suppressive effect of insulin signaling pathways on EIIIA inclusion is consistent with work showing increased EIIIA expression and fibrotic responses in type II diabetes^{4,5}. The enrichment of RIG-I-like signaling pathway genes among those required for highest EIIIA inclusion was also interesting, as fibrosis can be an important secondary component of viral responses. In addition, EIIIA is a damage-associated molecular pattern (DAMP) and EIIIA can activate TLR4, a critical signal in the induction of immune responses^{42,43}. Thus, EIIIA induction by RIG-I-like pathway activation in the endothelium could contribute to key anti-viral immune responses, such as the generation of memory cells. Future work will be required to assess the specific contributions of these pathways to EIIIA inclusion in vivo, and, conversely, the involvement of EIIIA splicing in the fibrotic and immune responses of these diseases.

In conclusion, we have demonstrated that the direct detection of splice isoforms can be used to identify regulators of alternative splicing in CRISPR screens. Using this approach, we have performed the first genome-wide screen for regulators of FN-EIIIA, revealing candidate pathways in the regulation of EIIIA inclusion and fibrotic responses in endothelial cells.

Materials and methods

Isolation and immortalization of mouse aortic endothelial cells (mAECs). Mouse aortic endothelial cells were isolated from FnAB-null and -het mice as described in Murphy et al.¹⁹. Cells were then sorted by flow cytometry (FACs) (BD Aria) on acetylated LDL+ and endothelial cell markers Icam2+ and Cd31+. After expansion, endothelial cells were immortalized by lentiviral TetOn-SV40 using the VSVG packaging plasmid. Cells were grown in low glucose DMEM and 10% FBS under 3% O₂ conditions using 2 µg/mL doxycycline (Dox).

Generation and amplification of CRISPR plasmid pools. (Splice factor pool) Five CRISPR-KO guide sequences were designed to each of 57 splice factor targets using described rules (Azimuth 2.0)³³. Oligos were ordered and BsmBI batch cloned into the gRNA expression cassette of a LentiCRISPR_v2 plasmid containing Cas9 (Addgene 52961). The library was amplified in Stb13 (Thermo) and tested by miSeq analysis for coverage and skew. Individual guides (e.g. to Rbfox2) followed the same protocol, but were confirmed by sanger sequencing. (Genome-wide pool) For the genome wide screen, the Brie library in LentiCRISPR_v2 (Addgene 73632) was obtained as a plasmid library and amplified in Stb14 (Thermo) on 500 cm².

LB-agar coated ampicillin + selection plates. The library was tested by NextSeq analysis for coverage and skew.

Transduction of splice factor pool and genome-wide CRISPR pool into mAECs. Lentivirus was generated in 293 T cells using delta 8.9⁴⁴ and pHCMV-EcoEnv (Addgene 15802)⁴⁵ as packaging plasmids and 25 kDa linear PEI as a transfection agent. Media was changed at 1 day and supernatant was taken at 3 days after transfection for the treatment of recipient cells at MOI < 0.3 (> 1000 infected cells per guide). Virus supernatant was added to recipient mAECs with polybrene (8 µg/mL), and cells were selected with puromycin for 4 days, confirming a MOI < 0.3 and complete killing of uninfected cells. An aliquot of cells was taken 3–4 days post infection for an early timepoint analysis of lentiviral library representation.

PrimeFlow detection of alternative splicing isoforms. mAECs harboring CRISPR guides were trypsinized and split into low glucose DMEM and 10% FBS into new dishes, without doxycycline to stop growth. 24 h later, cells were once again trypsinized and collected for PrimeFlow. Protocol for RNA detection was followed, according to manufacturer's instructions (ThermoFisher, see "Extended methods" section in Supplementary Information). Protocol was completed over the course of 2 days, using the stopping points described. Target probes were Alexa Fluor 488 for Fibronectin and Alexa Fluor 647 for either EIIIA or EIIIB (see "Extended methods" section in Supplementary Information). FnAB-null cells were included as a control for staining.

Reagent type	Description	Source
Vector	LentiCRISPR_v2	Addgene
Packaging plasmid	Delta 8.9	
Packaging plasmid	CMV-Eco	Addgene
CRISPR pool	Mouse genome-wide CRISPR pool	Addgene
Commercial kit	PrimeFlow RNA detection kit	ThermoFisher
Commercial kit	Quick DNA kit	Zymo
Commercial kit	Gel cleanup kit	Zymo
Software, algorithm	Mageck-0.5.6	SourceForge
Bacterial cells	Stbl3 (targeted screen)	ThermoFisher
	Stbl4 (Brie genome-wide screen)	
Commercial kit	RNAeasy minicolumns	Qiagen
qPCR reagent	iQ SYBR green supermix	BioRad
Mouse aortic endothelial cells	Isolated from FNab-het and FNab-null mice, as described in “Materials and methods” section	

Table 1. Key resources table.

Enrichment of guides in cells with increased or decreased EIIIA or EIIIB inclusion. mAECs with PrimeFlow staining were sorted based on the ratio of EIIIA or EIIIB to total FN, as a measure of inclusion frequency. Samples were digested overnight with Proteinase K at 55 °C, and DNA collected by Quick DNA kit (Zymo). For the genome-wide screen, at least 3 replicates were taken from each condition (see SI Table S1), and isolated independently. Lentiviral insertions in genomic DNA were amplified by nested PCR, using PCR1 primers (see SI Table S2) followed by PCR2 primers containing barcodes and Illumina priming sequences (see SI Table S2). PCR reactions were separated using a 2% agarose gel, and bands of interest were excised. PCR products were column cleaned (Gel cleanup kit, Zymo), and pooled based on relative concentration. Pooled samples were sequenced on Illumina NextSeq instrument using 75 bp single end (SE) reads (Table 1).

Identification of top Fn-EIIIA regulators (bioinformatics approach). Fastq files were analyzed using Mageck-0.5.6 software³², providing counts of each guide in each sequenced population, and differences in their representation (mageck test).

RNA extraction and qPCR. RNA extraction was performed using the Qiagen RNAeasy minicolumns, following the protocol provided by the manufacturer (including DNase treatment), and eluting in 10 uL of DNase, RNase free water. RNA concentrations were spot-checked (ThermoFisher, Nanodrop 2000) to ensure the RNA extraction was successful. cDNA was prepared using random primers and qPCR was run using BioRad’s iQ SYBR Green Supermix. For the analysis of EIIIA and EIIIB inclusion by qPCR, samples were extracted using the Qiagen FFPE extraction kit. qPCR was performed on random primed cDNA, as previously described (see SI Table S2 for qPCR primers)¹².

Cytokine and poly:IC treatment of cells. TetOn-SV40 immortalized mouse aortic endothelial cells were split into 96 well plates and taken off doxycycline (day 0). 24 h later (day 1), once the cells have stopped proliferating, the cells were treated with TNF α (10 ng/mL), IL-1 β (10 ng/mL), and IFN γ (500 units/mL). 24 h after cells were treated with the cytokines (day 2), they were treated with Poly(IC) (50 ug/mL). RNA was harvested in trizol 24 h after the addition of Poly(IC).

Ethics approval and consent to participate. No animals were used in this work. Cell lines used were previously published, and new data analysis on animal models used previously published data.

Data availability

Data from CRISPR screens are included as supplemental information (SI Table S3).

Received: 5 May 2021; Accepted: 14 September 2021

Published online: 06 October 2021

References

1. Astrof, S. & Hynes, R. O. Fibronectins in vascular morphogenesis. *Angiogenesis* **12**, 165–175 (2009).
2. Peters, J. H. *et al.* Plasma levels of fibronectin bearing the alternatively spliced EIIIB segment are increased after major trauma. *J. Lab. Clin. Med.* **141**, 401–410 (2003).
3. Peters, J. H., Maunder, R. J., Woolf, A. D., Cochrane, C. G. & Ginsberg, M. H. Elevated plasma levels of ED1+ (‘cellular’) fibronectin in patients with vascular injury. *J. Lab. Clin. Med.* **113**, 586–597 (1989).
4. Kanters, S. D. *et al.* Plasma levels of cellular fibronectin in diabetes. *Diabetes Care* **24**, 323–327 (2001).
5. Roy, S., Cagliero, E. & Lorenzi, M. Fibronectin overexpression in retinal microvessels of patients with diabetes. *Investig. Ophthalmol. Vis. Sci.* **37**, 258–266 (1996).

6. Ffrench-Constant, C., Van de Water, L., Dvorak, H. F. & Hynes, R. O. Reappearance of an embryonic pattern of fibronectin splicing during wound healing in the adult rat. *J. Cell Biol.* **109**, 903–914 (1989).
7. Chang, M. L., Chen, J. C., Alonso, C. R., Kornblihtt, A. R. & Bissell, D. M. Regulation of fibronectin splicing in sinusoidal endothelial cells from normal or injured liver. *Proc. Natl. Acad. Sci. U.S.A.* **101**, 18093–18098 (2004).
8. Astrof, S., Crowley, D. & Hynes, R. O. Multiple cardiovascular defects caused by the absence of alternatively spliced segments of fibronectin. *Dev. Biol.* **311**, 11–24 (2007).
9. Turner, C. J., Badu-Nkansah, K. & Hynes, R. O. Endothelium-derived fibronectin regulates neonatal vascular morphogenesis in an autocrine fashion. *Angiogenesis* **20**, 519–531 (2017).
10. Al-Yafeai, Z. *et al.* Endothelial FN (Fibronectin) deposition by alpha5beta1 integrins drives atherogenic inflammation. *Arter. Thromb. Vasc. Biol.* **38**, 2601–2614 (2018).
11. Chen, D. *et al.* Fibronectin signals through integrin alpha5beta1 to regulate cardiovascular development in a cell type-specific manner. *Dev. Biol.* **407**, 195–210 (2015).
12. Murphy, P. A. & Hynes, R. O. Alternative splicing of endothelial fibronectin is induced by disturbed hemodynamics and protects against hemorrhage of the vessel wall. *Arter. Thromb. Vasc. Biol.* **34**, 2042–2050 (2014).
13. Chauhan, A. K. *et al.* Prothrombotic effects of fibronectin isoforms containing the EDA domain. *Arter. Thromb. Vasc. Biol.* **28**, 296–301 (2008).
14. Dhanesha, N. *et al.* Genetic ablation of extra domain A of fibronectin in hypercholesterolemic mice improves stroke outcome by reducing thrombo-inflammation. *Circulation* **132**, 2237–2247 (2015).
15. Muro, A. F. *et al.* Regulated splicing of the fibronectin EDA exon is essential for proper skin wound healing and normal lifespan. *J. Cell Biol.* **162**, 149–160 (2003).
16. Jarnagin, W. R., Rockey, D. C., Koteliensky, V. E., Wang, S. S. & Bissell, D. M. Expression of variant fibronectins in wound healing: Cellular source and biological activity of the EIIIA segment in rat hepatic fibrogenesis. *J. Cell Biol.* **127**, 2037–2048 (1994).
17. Muro, A. F. *et al.* An essential role for fibronectin extra type III domain A in pulmonary fibrosis. *Am. J. Respir. Crit. Care Med.* **177**, 638–645 (2008).
18. Arslan, F. *et al.* Lack of fibronectin-EDA promotes survival and prevents adverse remodeling and heart function deterioration after myocardial infarction. *Circ. Res.* **108**, 582–592 (2011).
19. Murphy, P. A. *et al.* Alternative RNA splicing in the endothelium mediated in part by Rbfox2 regulates the arterial response to low flow. *Elife*. <https://doi.org/10.7554/eLife.29494> (2018).
20. George, J. *et al.* Transforming growth factor-beta initiates wound repair in rat liver through induction of the EIIIA-fibronectin splice isoform. *Am. J. Pathol.* **156**, 115–124 (2000).
21. Srebrow, A., Blaustein, M. & Kornblihtt, A. R. Regulation of fibronectin alternative splicing by a basement membrane-like extracellular matrix. *FEBS Lett.* **514**, 285–289 (2002).
22. Inoue, T., Nabeshima, K., Shimao, Y. & Koono, M. Hepatocyte growth factor/scatter factor (HGF/SF) is a regulator of fibronectin splicing in MDCK cells: Comparison between the effects of HGF/SF and TGF-beta1 on fibronectin splicing at the EDA region. *Biochem. Biophys. Res. Commun.* **260**, 225–231 (1999).
23. Blaustein, M. *et al.* Concerted regulation of nuclear and cytoplasmic activities of SR proteins by AKT. *Nat. Struct. Mol. Biol.* **12**, 1037–1044 (2005).
24. Blaustein, M. *et al.* Mammary epithelial-mesenchymal interaction regulates fibronectin alternative splicing via phosphatidylinositol 3-kinase. *J. Biol. Chem.* **279**, 21029–21037 (2004).
25. Bordeleau, F. *et al.* Tissue stiffness regulates serine/arginine-rich protein-mediated splicing of the extra domain B-fibronectin isoform in tumors. *Proc. Natl. Acad. Sci. U.S.A.* **112**, 8314–8319 (2015).
26. Cramer, P. *et al.* Coupling of transcription with alternative splicing: RNA pol II promoters modulate SF2/ASF and 9G8 effects on an exonic splicing enhancer. *Mol. Cell* **4**, 251–258 (1999).
27. Phanish, M. K. *et al.* The regulation of TGFbeta1 induced fibronectin EDA exon alternative splicing in human renal proximal tubule epithelial cells. *J. Cell Physiol.* **230**, 286–295 (2015).
28. Lim, L. P. & Sharp, P. A. Alternative splicing of the fibronectin EIIIB exon depends on specific TGCATG repeats. *Mol. Cell Biol.* **18**, 3900–3906 (1998).
29. Jangi, M., Boutz, P. L., Paul, P. & Sharp, P. A. Rbfox2 controls autoregulation in RNA-binding protein networks. *Genes Dev.* **28**, 637–651 (2014).
30. Joung, J. *et al.* Genome-scale CRISPR-Cas9 knockout and transcriptional activation screening. *Nat. Protoc.* **12**, 828–863 (2017).
31. Sanjana, N. E., Shalem, O. & Zhang, F. Improved vectors and genome-wide libraries for CRISPR screening. *Nat. Methods* **11**, 783–784 (2014).
32. Li, W. *et al.* MAGeCK enables robust identification of essential genes from genome-scale CRISPR/Cas9 knockout screens. *Genome Biol.* **15**, 554 (2014).
33. Doench, J. G. *et al.* Optimized sgRNA design to maximize activity and minimize off-target effects of CRISPR-Cas9. *Nat. Biotechnol.* **34**, 184–191 (2016).
34. Moore, B. B. & Moore, T. A. Viruses in idiopathic pulmonary fibrosis. Etiology and exacerbation. *Ann. Am. Thorac. Soc.* **12**, S186–S192 (2015).
35. Washburn, M. L. *et al.* A humanized mouse model to study hepatitis C virus infection, immune response, and liver disease. *Gastroenterology* **140**, 1334–1344 (2011).
36. Zaitoun, A. M. *et al.* Quantitative assessment of fibrosis and steatosis in liver biopsies from patients with chronic hepatitis C. *J. Clin. Pathol.* **54**, 461–465 (2001).
37. Werkman, I. *et al.* TLR3 agonists induce fibronectin aggregation by activated astrocytes: a role of pro-inflammatory cytokines and fibronectin splice variants. *Sci. Rep.* **10**, 532 (2020).
38. Xiao, R. *et al.* Pervasive chromatin-RNA binding protein interactions enable RNA-based regulation of transcription. *Cell* **178**, 107–121 (2019).
39. Lovci, M. T. *et al.* Rbfox proteins regulate alternative mRNA splicing through evolutionarily conserved RNA bridges. *Nat. Struct. Mol. Biol.* **20**, 1434–1442 (2013).
40. Stoilov, P., Lin, C. H., Damoiseaux, R., Nikolic, J. & Black, D. L. A high-throughput screening strategy identifies cardiotoxic steroids as alternative splicing modulators. *Proc. Natl. Acad. Sci. U.S.A.* **105**, 11218–11223 (2008).
41. Lai, C., Stepniak, D., Sias, L. & Funatake, C. A sensitive flow cytometric method for multi-parametric analysis of microRNA, messenger RNA and protein in single cells. *Methods* **134–135**, 136–148 (2018).
42. Julier, Z. *et al.* Fibronectin EDA and CpG synergize to enhance antigen-specific Th1 and cytotoxic responses. *Vaccine* **34**, 2453–2459 (2016).
43. Julier, Z., Martino, M. M., de Titta, A., Jeanbart, L. & Hubbell, J. A. The TLR4 agonist fibronectin extra domain A is cryptic, exposed by elastase-2; use in a fibrin matrix cancer vaccine. *Sci. Rep.* **5**, 8569 (2015).
44. Root, D. E., Hacohen, N., Hahn, W. C., Lander, E. S. & Sabatini, D. M. Genome-scale loss-of-function screening with a lentiviral RNAi library. *Nat. Methods* **3**, 715–719 (2006).
45. Sena-Esteves, M., Tebbets, J. C., Steffens, S., Crombleholme, T. & Flake, A. W. Optimized large-scale production of high titer lentivirus vector pseudotypes. *J. Virol. Methods* **122**, 131–139 (2004).

Acknowledgements

We are grateful for the help of Christopher (“Kit”) Bonin and Geneva Hargis in the UCONN Medical Science Writing group for editing.

Author contributions

P.M. developed the study concept and design; P.M. performed development of methodology. P.M. and J.H. wrote, reviewed and revised the paper; P.M., J.H., B.H. and A.K. provided acquisition of data. P.M. provided analysis and interpretation of data, and statistical analysis; P.M., J.H., B.H., A.K., E.J. and B.R. provided technical and material support. All authors read and approved the final paper.

Funding

University of Connecticut, School of Medicine startup funds and National Institutes of Health, NHLBI grant to PAM (K99/R00-HL125727).

Competing interests

The authors declare no competing interests.

Additional information

Supplementary Information The online version contains supplementary material available at <https://doi.org/10.1038/s41598-021-99079-1>.

Correspondence and requests for materials should be addressed to P.A.M.

Reprints and permissions information is available at www.nature.com/reprints.

Publisher’s note Springer Nature remains neutral with regard to jurisdictional claims in published maps and institutional affiliations.



Open Access This article is licensed under a Creative Commons Attribution 4.0 International License, which permits use, sharing, adaptation, distribution and reproduction in any medium or format, as long as you give appropriate credit to the original author(s) and the source, provide a link to the Creative Commons licence, and indicate if changes were made. The images or other third party material in this article are included in the article’s Creative Commons licence, unless indicated otherwise in a credit line to the material. If material is not included in the article’s Creative Commons licence and your intended use is not permitted by statutory regulation or exceeds the permitted use, you will need to obtain permission directly from the copyright holder. To view a copy of this licence, visit <http://creativecommons.org/licenses/by/4.0/>.

© The Author(s) 2021